Placental Malaria Induces a Unique Placental Methylation Profile Associated with Fetal Growth Restriction

Nida Ozarslan[1,2], Corina Mong[1,2], John Ategeka[3], Lin Li[1,2], Sirirak Buarpung[1,2], Joshua F. Robinson[2], Jimmy Kizza[3], Abel Kakuru[3], Moses R. Kamya[3,4], Grant Dorsey[5], Philip J. Rosenthal[5], Stephanie L. Gaw[1,2]*

[1]Division of Maternal-Fetal Medicine, Department of Obstetrics, Gynecology & Reproductive Sciences, University of California, San Francisco (UCSF); San Francisco, CA, USA.

[2] Center for Reproductive Sciences and Department of Obstetrics, Gynecology, and Reproductive Sciences, University of California, San Francisco (UCSF); San Francisco, CA, USA.

[3] Infectious Diseases Research Collaboration; Uganda.

[4] Department of Medicine, Makerere University; Kampala, Uganda.

[5] Division of HIV, Global Medicine, and Infectious Diseases, Department of Medicine, University of California, San Francisco; San Francisco, CA, USA.

Keywords: pregnancy, placenta, malaria in pregnancy, epigenetics, EPIC array, DNA methylation, human, microarray, EWAS, FGR, IUGR, fetal programming, DoHAD

* Correspondence:

Stephanie L. Gaw, MD, PhD
Associate Professor
Division of Maternal-Fetal Medicine
Center for Reproductive Sciences
Department of Obstetrics, Gynecology and Reproductive Sciences
University of California, San Francisco
513 Parnassus Ave, Box 0556 16HSE
San Francisco, CA 94143
E-mail: Stephanie.Gaw@ucsf.edu

Abstract: (216/350 words)

Background: Fetal growth restriction (FGR) is associated with perinatal death and other adverse birth outcomes, as well as long term complications including increased childhood morbidity, abnormal neurodevelopment, and cardio-metabolic diseases in adulthood. FGR has been associated with placental epigenetic reprogramming, which may mediate these long term outcomes. Placental malaria (PM) is the leading cause of FGR globally, but the impact on placental epigenetics is unknown. We hypothesized that methylomic profiling of placentas from non-malarial and malarial FGR would reveal common and distinct mechanistic pathways associated with FGR.

Results: We used a methylation array to compare the CpG profiles between FGR from a cohort with no malaria exposure and a cohort of pregnancies complicated by both PM and FGR. Non-malarial FGR was associated with 65 differentially methylated CpGs, whereas PM-FGR was associated with 133 DMCs, compared to their corresponding controls. One DMC (cg16389901) was commonly hypomethylated in both groups, corresponding to the promoter region of *BMP4*. Comparison of FGR vs. PM-FGR identified 522 DMCs between these two groups, which was not attributable to geographic location or different cellular compositions of these two groups.

Conclusion: Placentas from pregnancies with PM-associated FGR showed distinct methylation profiles as compared to non-malarial FGR, suggesting novel epigenetic reprogramming in response to malaria. There may be distinct long-term health outcomes in FGR pregnancies also complicated by PM.

Background

Malaria in pregnancy leads to various adverse outcomes including fetal growth restriction (FGR). low birth weight, preterm birth, and fetal loss. The WHO reports that in 2021, 34% of pregnant individuals in sub-Saharan Africa were exposed to malaria which resulted in 819,000 babies born with low birth weight. Placental malaria (PM), characterized by the sequestration of parasite-infected red blood cells in the placental intervillous spaces, is the leading global cause of FGR and has been associated with small for gestational age and worse neurodevelopmental outcomes (1–4). PM may lead to FGR through multiple mechanisms. Congestion and inflammation secondary to sequestration of infected RBC in the intervillous spaces during pregnancy disrupts trophoblast invasion and angiogenesis, decreasing umbilical artery flow and subsequently to FGR (5–7). Vascular dysfunction and chronic inflammation may contribute to impaired nutrient exchange at the fetal-maternal interface and imbalances in the growth factors (8).

Fetal growth, as measured by ultrasound-estimated fetal weight for gestational age, has important influences on human health. Early onset FGR (<32 weeks gestation) and severe FGR (<3rd percentile) are associated with up to 1.5-fold increased risk of stillbirth and a 2 to 5-fold risk of perinatal death (9). Long term complications of FGR include increased childhood morbidity, and even cardiovascular, metabolic, and neuropsychiatric diseases in adulthood (2,4,10–22). Non-malarial etiologies of FGR include maternal comorbidities, placental dysfunction, genetics, and environmental exposures (e.g. tobacco smoke) (23).

Separate fields of research have demonstrated that PM and FGR independently impact infant growth and neurodevelopment (24–28). These long-term health impacts may be mediated through epigenetic modifications, including DNA methylation, histone marks, and non-coding RNAs. In FGR, placental epigenetic modifications in genes related to cellular growth, nutrient transport, and inflammatory responses have been described (29–33). Epigenetic studies of human responses to malaria have been largely focused on immune markers of disease susceptibility (34,35). Altered DNA methylation has been demonstrated in monocytes after malaria infection, resulting in age-dependent changes in innate immune and inflammatory responses (36,37). There is no data on placental epigenetic reprogramming after malaria in pregnancy.

In this study we aimed to identify whether non-malaria FGR is associated with similar methylation profiles as PM-associated FGR. This data is important to understand the shared and divergent mechanisms of fetal programming in PM and FGR.

Methods

Study design and subjects

Placental samples were collected from two independent patient cohorts to investigate the placental methylation levels in malarial and non-malarial FGR. Cohort 1 (no malaria) was comprised of placental samples prospectively collected at the University of California, San Francisco from 2018 to 2022. (IRB #10-00505, #20-32077 and #21-33986). Cohort 2 (malaria endemic) was comprised of placental samples prospectively collected from 2021-2022 in Busia, Uganda, as part of an ongoing randomized-controlled trial of intermittent preventative treatment for malaria in pregnancy (NCT04336189, IRB#19-29105).

Case definitions: All patients were primigravidas and had no evidence of fetal genetic or structural anomalies. FGR cases were identified by estimated fetal weight < 10%ile for gestational age on all prenatal ultrasounds throughout pregnancy (up to 4) and birth weight <10%ile for gestational age by Intergrowth-21 birth weight standards (38). PM-FGR cases were complicated by both FGR and placental malaria (PM) diagnosed by placental histopathology. Control cases from each cohort were from healthy pregnancies with no pregnancy complications and no evidence of malaria in pregnancy at any time during the study (for Cohort 2). Cases were divided into four groups: 1) FGR (no malaria, n=8), 2) C^{FGR} (healthy controls from the United States, n=4), 3) PM-FGR (placental malaria and FGR, n=8), and 4) $C^{PM\text{-}FGR}$ (healthy controls from Uganda, n=4) (**Figure 1A**. Detailed case information is provided in **Table 1.**

Specimen collection

Placental biopsies were collected from the maternal side of the placenta within 1 hour of delivery. Biopsies no larger than 5 x 10 x 10mm were washed with ice-cold PBS three times and placed in RNAlater™ (Qiagen, Germantown, MD). After a minimum incubation of 24 hours in RNAlater at 4°C, biopsies were frozen and stored at -80°C.

100 DNA extraction

101 DNeasy Blood & Tissue Kit (Qiagen, Germantown, MD) was used according to the manufacturer's
102 standard protocol to extract DNA from placental biopsies. Samples were treated with RNase for 2
103 minutes. Infinite M NanoQuant (Tecan, Morrisville, NC) was used to estimate the purity and concentration
104 of extractive DNA. The A260/A280 ratio for all samples was between 1.75-1.93.

105 Illumina Infinium MethylationEPIC v1 assay

106 Methylation levels were assessed using Infinium Methylation EPIC v1.0 (Illumina, San Diego, CA) assay
107 following the manufacture's protocol. The EZ DNA Methylation-Lightning Kit (Zymo Research, Irvine, CA)
108 following the standard protocol was used for bisulfite conversion. Briefly, bisulfite conversion was
109 performed on genomic DNA. Bisulfite converted DNA was amplified and fragmented. DNA was
110 precipitated and resuspended before hybridizing to the BeadChip. After hybridization, BeadChip was
111 washed to remove any unspecific binding, extended and stained primers before BeadChip was ready for
112 imaging using iScan (Illumina, San Diego, CA) platform.

113 Bioinformatic analysis

114 The raw data obtained from the iScan platform was cleaned and preprocessed for data analysis using R
115 (version 4.2.1) and minfi package (version 1.44.0). The quality of the samples was assessed by
116 computing detection p-values for all probes. The samples which exhibit a detection p-value higher than
117 0.05 in at least 10% of all the probes was excluded from the analysis. Data preprocessing was performed
118 using the quantile normalization method. Low-quality probes that failed at a detection p-value of 0.05 in at
119 least 10% of the samples, probes located on the sex chromosome (X and Y), probes with SNPs at the
120 CpG site, and cross-reactive probes were filtered out prior to differential methylation analysis. No samples
121 were excluded based on high p-value probes. The total number of probes before filtering was 865,859,
122 whereas total number of probes after filtering was 786,227.

123 Differential methylation analysis was performed using M values (log-ratio of methylated and unmethylated
124 signals) of methylation by limma (version 3.54.2) implemented in the minfi package, replacing expression
125 levels with M values in the data analysis process. β-value was used to represent the methylation levels of

126 all the probes. Differentially methylated CpGs were identified based on an unadjusted *p*-value < 0.0001
127 and absolute difference in mean methylation (|Δβ|) > 10% (test group vs. control group). Target gene
128 name was identified based on UCSC database and functional enrichment analysis was conducted using
129 DAVID.

130 Cellular deconvolution analysis was conducted using *planet* (v1.12) package on R (39). Figures were
131 generated using R Studio (v2023.03.0+386), GraphPad Prism (v10.2.3) and BioRender.

132 **Results**

133 Dimensional reduction analysis

134 The methylation levels of >850,000 CpG sites were detected using Illumina Infinium MethylationEPIC
135 Array v1 for 24 placentas. We identified 786,227 CpG sites after applying quality control measures as
136 described above. First, principal component analysis was applied using the M-values of all CpG sites to
137 understand the influence of FGR, placental malaria-FGR (PM-FGR) or geographic location on the overall
138 methylation profiles (**Figure 1**). We did not observe any distinct separation between the four groups:
139 FGR, PM-FGR, C^{FGR} and $C^{PM\text{-}FGR}$ (**Figure 1B**) or among any of the pairwise comparisons based on FGR
140 status or collection site (**Figure 1C-E**). Separation was most prominent between FGR and PM-FGR
141 groups (**Figure 1F**).

142 Identification of Differentially Methylated CpGs (DMCs)

143 We investigated the specific changes in placental methylation levels observed with non-malarial and
144 placental malarial FGR. To capture a broader range of differentially methylated CpG sites, we used an
145 unadjusted p value cutoff of p<0.0001 and a secondary cutoff of at least 10% absolute difference in mean
146 methylation (|Δβ| > 0.10). To confirm the power of the significance cutoff in terms of differentiating the
147 groups, unsupervised hierarchical clustering was performed using β-values of the respective DMCs. As
148 expected, our samples clustered based on study group (**Supplemental Figure 1, Supplemental Table**
149 **1**).

150 Changes observed with non-malarial FGR

151 We first investigated the influence of non-malarial FGR on placental methylation profiles. The overall

152 distribution of CpG sites with a $p<0.0001$ was equally distributed across all 22 autosomal chromosomes
153 (**Figure 2A**). Between FGR vs. C^{FGR}, 65 CpG sites were differentially methylated ($p<0.0001$ and
154 $|\Delta\beta|>0.1$), of which 17 were hypermethylated and 48 were hypomethylated with FGR (**Figure 2B**).
155 Functional enrichment analysis using the genes linked to those 65 DMCs showed that the CpGs
156 hypermethylated with non-malarial FGR were associated with genes related to negative regulation of
157 signaling. In contrast, hypomethylated CpGs were associated with genes related to response to stimulus,
158 suggesting an overall activation to cellular signals in FGR placenta.

159 <u>Changes observed with placental malaria and FGR</u>
160 To identify the changes observed with placental malaria and FGR, we compared methylation levels of
161 CpG sites between PM-FGR vs. $C^{PM\text{-}FGR}$. The overall distribution of CpG sites with a $p<0.0001$ were
162 homogenous across all 22 autosomal chromosomes (**Figure 2C**). Between PM-FGR vs.
163 $C^{PM\text{-}FGR}$, 133 CpGs were differentially methylated ($p<0.0001$ and $|\Delta\beta|>0.1$); of these, 51 were
164 hypermethylated and 82 were hypomethylated with PM-FGR (**Figure 2D**). Functional enrichment analysis
165 was conducted using the genes linked to these 133 DMCs. The CpGs hypermethylated with PM-FGR
166 were associated with genes related to developmental processes, whereas the hypomethylated CpGs
167 were associated with genes related to stimulus response.

168 <u>Common changes observed with non-malarial FGR and PM-FGR</u>
169 To identify the epigenetic modulations observed with both non-malarial and PM-FGR, we investigated the
170 overlapping DMCs between FGR vs. C^{FGR} and PM-FGR vs. $C^{PM\text{-}FGR}$ comparisons. We identified only a
171 single CpG, cg16389901, that was commonly hypomethylated with both FGR and PM-FGR when
172 compared to their respective controls (**Figure 3A**). The cg16389901site is in the promoter region of two
173 splice variants of *BMP4*, a cell growth-related gene known to participate in trophoblast differentiation
174 within the placenta (40) (**Figure 3B**). DNA methylation levels of other CpGs associated with *BMP4* did not
175 show a difference between FGR vs. C^{FGR} or PM-FGR vs. $C^{PM\text{-}FGR}$ comparisons.

176 <u>Differentially methylated CpGs between non-malarial FGR vs. placental malarial FGR</u>
177 We next compared the methylation profiles between FGR and PM-FGR. The distribution of CpGs with

178 $p<0.0001$ was equal across all 22 autosomal chromosomes (**Figure 4A**). There was a higher number of
179 CpG sites (529 CpGs) with a $p<0.0001$ and $|\Delta\beta|>0.1$ cutoff between FGR vs. PM-FGR (**Figure 4B**) when
180 compared to FGR vs. C^{FGR} (**Figure 2B)** or PM-FGR vs. $C^{PM\text{-}FGR}$ (**Figure 2D**), highlighting the distinct
181 changes observed with placental malaria. To account for baseline epigenetic differences based on the
182 distinct geographical locations of the two cohorts, we compared the DMCs between our two control
183 groups (C^{FGR} vs. $C^{PM\text{-}FGR}$), which 183 CpGs that were differentially methylated between the two study
184 sites. Of these 183 DMCs, 7 CpG sites were also identified when comparing FGR vs. PM-FGR. Exclusion
185 of these 7 CpGs as potentially affected by population-based differences resulted in 522 CpGs that were
186 impacted by PM status (**Figure 4C**). Of these, 143 were hypermethylated in FGR placenta, and 379 were
187 hypermethylated in PM-FGR placenta. The CpGs hypermethylated with FGR were associated with genes
188 related to cellular developmental processes. With FGR, 3 CpG sites in the promoter region of *ARPC1B*
189 and 4 CpG sites in the promoter region of *ZSCAN23* were hypermethylated. CpGs hypermethylated with
190 PM-FGR were associated with genes related to metabolic processes. On the other hand, 7 CpG sites in
191 the promoter region of *FAM124B* and 4 CpG sites in the promoter region of *SPG7* were hypermethylated
192 with PM-FGR.

193 <u>Identifying the cellular composition of all placental samples</u>

194 Our study used DNA extracted from homogenized placental tissue, combining various cell types as a
195 single sample. To understand the estimated cellular composition of each sample, we performed cellular
196 deconvolution analysis based on reference methylation data of term placental cells generated by Yuan et
197 al. (39) (**Figure 5A**). Robust partial correlations (RPC) method was used to identify the percentage of
198 syncytiotrophoblast, trophoblasts, endothelial cells, stromal cells, Hofbauer cells and nucleated red blood
199 cells (nRBC) based on β-values of the most distinguishing CpG sites among these cell types. Our
200 samples demonstrated a high proportion of syncytiotrophoblast, constituting an average of 69.5%. The
201 next most prevalent cell types were stromal cells (13.9%), endothelial cells (12.1%) and trophoblasts
202 (3.8%). The average abundance of Hofbauer cells and nRBC in total was less than 0.6%. We performed
203 unsupervised hierarchical clustering to investigate whether the cellular composition of our samples was
204 leading to distinct separation between our four study groups (**Figure 5B**). Overall, the cellular composition
205 of our samples did not show any clear separation among groups (**Figure 5B, Supplemental Figure 2**).

206 Hierarchical clustering of only FGR and PM-FGR samples demonstrated distinct clustering between these
207 two groups (**Figure 5C**). This separation was primarily driven by the significant increase in the percentage
208 of syncytiotrophoblast in PM-FGR (%74.4) samples compared to FGR (%65.5) ($p<0.002$). Only a single
209 CpG site was overlapping with the 522 identified CpGs used for cellular deconvolution analysis, indicating
210 that DMCs identified between FGR vs. PM-FGR were not driven by differences in cellular composition
211 (**Figure 5D**).

212 **Discussion**

213 To our knowledge, this is the first study to investigate methylation profiles in PM. We found that
214 placentas from malaria and non-malaria FGR cases exhibited highly divergent methylation profiles.
215 Interestingly, there was only a single CpG site, associated with the promoter region of *BMP4* that was
216 commonly hypomethylated with both malarial and non-malarial FGR. In PM-FGR, hypermethylated CpGs
217 were associated with genes related to developmental processes whereas hypermethylated CpGs in FGR
218 were associated with genes related to metabolic processes. Cellular deconvolution demonstrated
219 differences in the relative abundances of placental cell types; however, these differences did not explain
220 the distinct methylation profiles between non-malarial and PM-FGR. These results suggest novel
221 epigenetic modifications in response to PM-FGR compared to non-malarial FGR.

222 Previous studies investigating placental epigenetic changes occurring with FGR have identified
223 various differentially methylated CpG sites and related genes involved with fatty acid oxidation,
224 transcriptional regulation, immune responses, cell adhesion, metabolism, cell growth (32,41–44). Our
225 results did not have any clear overlap between the most of these studies. This may be due to diverse
226 mechanisms of epigenetic modulation, as well as differences in study populations. Similar to our study,
227 one study from Korea investigating the methylation levels of placenta and cord blood samples with FGR
228 described changes in methylation profiles of genes related to metabolism and developmental pathways
229 (43).

230 Both non-malarial FGR and PM-FGR are independently associated with moderate numbers of
231 differentially methylated CpGs when compared to their corresponding controls. Interestingly, a single CpG

site was commonly hypomethylated with both non-malarial and PM-FGR—cg16389901. This site is located 200-1500 bases upstream of the transcription start site of the *BMP4* gene. BMP4 is a well-known growth associated protein which also plays important role in trophoblast differentiation (40). The Korean study also described hypermethylation of the negative regulation of the BMP signaling pathway, which is aligns with our results (43). Hypomethylation of *BMP4*, resulting in increased expression, may be a common compensatory mechanism in the placenta to counteract other functional changes that lead to inhibited fetal growth.

Hypermethylated CpG sites with FGR compared to PM-FGR included CpGs located at the promoter regions of *ARPC1B* and *ZSCAN23*. Homozygous mutations in the *ARPC1B* gene have been associated with disruptions of the immune system (45). Promoter region hypermethylation of *ZSCAN23* has been associated with acceleration of pancreatic cancer growth (46). Hypermethylated CpG sites in PM-FGR compared to FGR included CpGs located at the promoter regions of *FAM124B* and *SPG7*. *FAM124B* has been proposed as an important protein involved in neurodevelopmental disorders while SpG7 mutations have been linked to spastic paraplegia and cerebellar ataxia (47,48). Further follow up studies on offspring are needed to investigate the long-term outcomes occurring with non-malarial FGR vs. PM-associated FGR and to understand whether these clinical outcomes are potentially mediated by these diverse epigenetic profiles.

Cellular deconvolution analysis revealed dominance of syncytiotrophoblasts, which had significantly higher proportions in PM-FGR samples. The increased proportion of syncytiotrophoblasts may be a consequence of syncytial knot formation commonly observed with PM, which is thought to be a response to inflammatory damage associated with infected RBC in the intervillous spaces (49). Despite the differences in cellular composition between non-malarial FGR and PM-FGR, the differentially methylated CpGs were distinct from those associated with specific cell types. In contrast, a study that conducted the same deconvolution analysis on placentas from monochorionic twins complicated by selective FGR found decreased proportions of stromal cells with FGR compared the normally grown twin (41). This suggests a distinct placental response to FGR in twins compared with singletons.

Our study has some limitations. First, this is a small sample size and larger studies are needed to confirm our findings. Due to the homogenization of placental tissue, we were also unable to distinguish the differences between cell types, particularly the maternal and fetal cells. Due to the high prevalence of malaria in pregnancy at our study site in Uganda, we were unable to identify any FGR cases from Uganda that did not have any evidence of malaria infection during pregnancy; these cases would provide a more accurate comparison for non-malarial and PM-FGR in a similar population. Finally, we have focused on methylation profiles detected by a targeted methylation array, rather than whole genome bisulfide sequencing which may identify additional differentially methylated CpGs. Further studies investigating other types of epigenetic mechanisms such as histone modifications or assessment of open chromatin regions would provide deeper insight into epigenetic changes occurring with non-malarial FGR and PM-FGR. Additional transcriptomic and proteomic analysis of similar cohorts would also reveal insight into downstream effects of epigenetic modifications.

The strengths of our study include detailed characterizations of the pregnancies, allowing for the selection of appropriate controls for each population. We only included primigravid patients to avoid confounding from gravidity-induced differences in methylation profiles. Finally, placental biopsies from both sites were collected and processed with the same protocol, allowing for comparison between the different patient populations.

The significant divergence in DMCs in FGR and PM-FGR, even after controlling for geographic location, suggests distinct pathways of epigenetic reprogramming in these two populations. Placental responses to malaria may have a strong influence on placental epigenetics, with potential implications for long-term health in the offspring.

Declarations

Ethics approval and consent to participate

This study was approved by the University of California, San Francisco and Makerere University. Written informed consent was obtained from all participants.

283 Availability of data and materials

284 The dataset generated during the study will available in the GEO repository (waiting for accession

285 number).

286 Competing interests

287 The authors declare that they have no competing interests.

288 Funding

289 This study was supported by the National Institutes of Health (NIAID K08AI141728 to SLG and

290 U01AI141308 to GD and PJR), and the Bill and Melinda Gates Foundation (INV-017035 to SLG).

291 Authors' contributions

292 Conceptualization: NO and SLG

293 Methodology: NO and SLG

294 Investigation: NO, CM, JA, LL, SB, JFR

295 Funding acquisition: MRK, GD, PJR, SLG

296 Project administration: AK, JK

297 Supervision: AK, SLG

298 Writing – original draft: NO and SLG

299 Writing – review & editing: All Authors

300 Acknowledgments

301 The authors thank all study participants. We also thank Keith Boohrer, Xiaojing Yang and Kai Chang from

302 the Zymo Research Corporation for their technical support.

303 **Figure and Table Legends**

304 **Table 1. Patient characteristics.** cHTN; chronic hypertension, gHTN; gestational hypertension, gDM;

305 gestational DM, PreE; preeclampsia, SIPE; superimposed preeclampsia.

306 **Figure 1. Principal Component Analysis. A.** Schematic demonstration of study groups and collection

307 sites. **B.** Principal component analysis including all samples. **C.** Principal component analysis of FGR and

308 C^{FGR} samples. **D.** Principal component analysis of PM-FGR and C^{PM-FGR} samples **E.** Principal component
309 analysis of C^{FGR} and C^{PM-FGR} samples **F**. Principal component analysis of FGR and PM-FGR samples.

310 **Figure 2. Differentially methylated CpGs (DMCs) observed with non-malarial FGR and placental**
311 **malaria associated FGR and their respective controls**. A. Manhattan plot of CpGs with a p-
312 value<0.0001 between FGR vs. C^{FGR} **B.** Volcano plot displaying DMCs between FGR vs. C^{FGR} in red
313 based on significance cutoff (p<0.0001 and |Δβ| > 0.1) **C.** Manhattan plot of CpGs with a p-value<0.0001
314 between PM-FGR vs. $^{CPM-FGR}$. **D**. Volcano plot displaying DMCs between PM-FGR vs. C^{PM-FGR} in red
315 based on significance cutoff (p<0.0001 and |Δβ| >0.1)

316 **Figure 3. Commonly differentially methylated CpG site with non-malarial FGR and placental**
317 **malarial FGR**. A. Venn diagram demonstrating the sole overlapping differentially methylated CpG site,
318 cg16138990, that was commonly hypomethylated with both non-malarial and placental malarial FGR
319 when compared to their controls. **B.** Average DNA methylation of CpG sites associated with BMP4,
320 including cg16138990 (marked in red), for all four groups. Red asterisk indicated significance.

321 **Figure 4. Differentially methylated CpGs (DMCs) observed between non-malarial FGR vs. placental**
322 **malaria associated FGR. A.** Manhattan plot of CpGs with a p-value<0.0001 between FGR vs. PM-FGR
323 **B.** Volcano plot displaying 529 CpGs with a p<0.0001 and |Δβ| >0.1 value between FGR vs. PM-FGR in
324 red based**. C.** Venn diagram demonstrating the 522 DMCs between FGR vs. PM-FGR after subtracting
325 geographical location-driven baseline differences.

326 **Figure 5. Cellular deconvolution analysis based on overall methylation levels. A.** Cell composition
327 of all samples estimated using robust partial correlations analysis through planet package in R. **B.**
328 Hierarchical clustering of all samples based on cellular deconvolution results. **C.** Hierarchical clustering of
329 FGR and PM-FGR samples based on cellular deconvolution analysis. **D.** Venn diagram demonstrating
330 the overlap between CpGs used for cellular deconvolution analysis and differentially methylated CpGs
331 between FGR vs. PM-FGR.

332 **Supplemental Figure 1. Hierarchical clustering of samples based on methylation levels of**

333 **differentially methylated CpGs (DMCs**). A. Methylation level of 65 DMCs between FGR vs. C^{FGR} **B.**

334 Methylation level of 133 DMCs between PM-FGR vs. $C^{PM\text{-}FGR}$ **C.** Methylation level of 183 DMCs between

335 C^{FGR} vs. $C^{PM\text{-}FGR}$ **D.** Methylation level of 522 DMCs between FGR vs. PM-FGR

336 **Supplemental Figure 2. Hierarchical clustering of samples based on cellular composition. A.**

337 Hierarchical clustering of FGR and C^{FGR} samples based on cellular composition**. B.** Hierarchical

338 clustering of PM-FGR and $C^{PM\text{-}FGR}$ samples based on cellular composition.

339 **Supplemental Table 1. List of differentially methylated CpG sites.**

340 **References**

341 1. Garrison A, Boivin MJ, Fiévet N, Zoumenou R, Alao JM, Massougbodji A, et al. The Effects of Malaria
342 in Pregnancy on Neurocognitive Development in Children at 1 and 6 Years of Age in Benin: A
343 Prospective Mother-Child Cohort. Clin Infect Dis Off Publ Infect Dis Soc Am. 2022 Mar 9;74(5):766–
344 75.

345 2. Bangirana P, Conroy AL, Opoka RO, Semrud-Clikeman M, Jang JH, Apayi C, et al. Effect of Malaria
346 and Malaria Chemoprevention Regimens in Pregnancy and Childhood on Neurodevelopmental and
347 Behavioral Outcomes in Children at 12, 24, and 36 Months: A Randomized Clinical Trial. Clin Infect
348 Dis. 2023 Feb 18;76(4):600–8.

349 3. Conroy AL, Bangirana P, Muhindo MK, Kakuru A, Jagannathan P, Opoka RO, et al. Case Report:
350 Birth Outcome and Neurodevelopment in Placental Malaria Discordant Twins. Am J Trop Med Hyg.
351 2019 Mar;100(3):552–5.

352 4. Bangirana P, Opoka RO, Boivin MJ, Idro R, Hodges JS, Romero RA, et al. Severe Malarial Anemia is
353 Associated With Long-term Neurocognitive Impairment. Clin Infect Dis. 2014 Aug 1;59(3):336–44.

354 5. Moore KA, Simpson JA, Wiladphaingern J, Min AM, Pimanpanarak M, Paw MK, et al. Influence of the
355 number and timing of malaria episodes during pregnancy on prematurity and small-for-gestational-
356 age in an area of low transmission. BMC Med. 2017 Dec;15(1):117.

357 6. Chua CLL, Khoo SKM, Ong JLE, Ramireddi GK, Yeo TW, Teo A. Malaria in Pregnancy: From
358 Placental Infection to Its Abnormal Development and Damage. Front Microbiol. 2021 Nov
359 11;12:777343.

360 7. Dorman EK, Shulman CE, Kingdom J, Bulmer JN, Mwendwa J, Peshu N, et al. Impaired
361 uteroplacental blood flow in pregnancies complicated by falciparum malaria: Uterine artery Doppler
362 and malaria. Ultrasound Obstet Gynecol. 2002 Feb;19(2):165–70.

363 8. Chandrasiri UP, Chua CLL, Umbers AJ, Chaluluka E, Glazier JD, Rogerson SJ, et al. Insight Into the
364 Pathogenesis of Fetal Growth Restriction in Placental Malaria: Decreased Placental Glucose
365 Transporter Isoform 1 Expression. J Infect Dis. 2014 May 15;209(10):1663–7.

366 9. Madden JV, Flatley CJ, Kumar S. Term small-for-gestational-age infants from low-risk women are at
367 significantly greater risk of adverse neonatal outcomes. Am J Obstet Gynecol. 2018
368 May;218(5):525.e1-525.e9.

369 10. Weckman AM, Conroy AL, Madanitsa M, Gnaneswaran B, McDonald CR, Kalilani-Phiri L, et al.
370 Neurocognitive outcomes in Malawian children exposed to malaria during pregnancy: An
371 observational birth cohort study. PLoS Med. 2021 Sep;18(9):e1003701.

372 11. Colella M, Frérot A, Novais ARB, Baud O. Neonatal and Long-Term Consequences of Fetal Growth
373 Restriction. Curr Pediatr Rev. 2018 Dec 21;14(4):212–8.

374 12. Lesseur C, Paquette AG, Marsit CJ. Epigenetic Regulation of Infant Neurobehavioral Outcomes. Med
375 Epigenetics. 2014 Jun 11;2(2):71–9.

376 13. Mericq V, Martinez-Aguayo A, Uauy R, Iñiguez G, Van Der Steen M, Hokken-Koelega A. Long-term
377 metabolic risk among children born premature or small for gestational age. Nat Rev Endocrinol. 2017
378 Jan;13(1):50–62.

379 14. D'Agostin M, Di Sipio Morgia C, Vento G, Nobile S. Long-term implications of fetal growth restriction.
380 World J Clin Cases. 2023 May 6;11(13):2855–63.

381 15. Chan PYL, Morris JM, Leslie GI, Kelly PJ, Gallery EDM. The Long-Term Effects of Prematurity and
382 Intrauterine Growth Restriction on Cardiovascular, Renal, and Metabolic Function. Int J Pediatr.
383 2010;2010:1–10.

384 16. Leon DA, Lithell HO, Vagero D, Koupilova I, Mohsen R, Berglund L, et al. Reduced fetal growth rate
385 and increased risk of death from ischaemic heart disease: cohort study of 15 000 Swedish men and
386 women born 1915-29. BMJ. 1998 Jul 25;317(7153):241–5.

387 17. Martyn CN, Barker DJ, Jespersen S, Greenwald S, Osmond C, Berry C. Growth in utero, adult blood
388 pressure, and arterial compliance. Heart. 1995 Feb 1;73(2):116–21.

389 18. Liefke J, Heijl C, Steding-Ehrenborg K, Morsing E, Arheden H, Ley D, et al. Fetal growth restriction
390 followed by very preterm birth is associated with smaller kidneys but preserved kidney function in
391 adolescence. Pediatr Nephrol Berl Ger. 2023 Jun;38(6):1855–66.

392 19. Senra JC, Yoshizaki CT, Doro GF, Ruano R, Gibelli MABC, Rodrigues AS, et al. Kidney impairment in
393 fetal growth restriction: three-dimensional evaluation of volume and vascularization. Prenat Diagn.
394 2020 Oct;40(11):1408–17.

395 20. Arigliani M, Stocco C, Valentini E, De Pieri C, Castriotta L, Ferrari ME, et al. Lung function between 8
396 and 15 years of age in very preterm infants with fetal growth restriction. Pediatr Res. 2021
397 Sep;90(3):657–63.

398 21. Nikolajev K, Heinonen K, Hakulinen A, Länsimies E. Effects of intrauterine growth retardation and
399 prematurity on spirometric flow values and lung volumes at school age in twin pairs. Pediatr
400 Pulmonol. 1998 Jun;25(6):367–70.

401 22. Grunnet LG, Bygbjerg IC, Mutabingwa TK, Lajeunesse-Trempe F, Nielsen J, Schmiegelow C, et al.
402 Influence of placental and peripheral malaria exposure in fetal life on cardiometabolic traits in adult
403 offspring. BMJ Open Diabetes Res Care. 2022 Apr;10(2):e002639.

404 23. ACOG Practice Bulletin No. 204: Fetal Growth Restriction. Obstet Gynecol. 2019 Feb;133(2):e97–
405 109.

24. Korzeniewski SJ, Allred EN, Joseph RM, Heeren T, Kuban KCK, O'Shea TM, et al. Neurodevelopment at Age 10 Years of Children Born <28 Weeks With Fetal Growth Restriction. Pediatrics. 2017 Nov 1;140(5):e20170697.

25. Leitner Y, Fattal-Valevski A, Geva R, Eshel R, Toledano-Alhadef H, Rotstein M, et al. Neurodevelopmental outcome of children with intrauterine growth retardation: a longitudinal, 10-year prospective study. J Child Neurol. 2007 May;22(5):580–7.

26. Murray E, Fernandes M, Fazel M, Kennedy S, Villar J, Stein A. Differential effect of intrauterine growth restriction on childhood neurodevelopment: a systematic review. BJOG Int J Obstet Gynaecol. 2015 Jul;122(8):1062–72.

27. Elgueta D, Murgas P, Riquelme E, Yang G, Cancino GI. Consequences of Viral Infection and Cytokine Production During Pregnancy on Brain Development in Offspring. Front Immunol. 2022 Apr 7;13:816619.

28. Sacchi C, Marino C, Nosarti C, Vieno A, Visentin S, Simonelli A. Association of Intrauterine Growth Restriction and Small for Gestational Age Status With Childhood Cognitive Outcomes: A Systematic Review and Meta-analysis. JAMA Pediatr. 2020 Aug 1;174(8):772.

29. Lapehn S, Paquette AG. The Placental Epigenome as a Molecular Link Between Prenatal Exposures and Fetal Health Outcomes Through the DOHaD Hypothesis. Curr Environ Health Rep. 2022 Apr 29;9(3):490–501.

30. Nawathe AR, Christian M, Kim SH, Johnson M, Savvidou MD, Terzidou V. Insulin-like growth factor axis in pregnancies affected by fetal growth disorders. Clin Epigenetics. 2016 Dec;8(1):11.

31. Lee MH, Jeon YJ, Lee SM, Park MH, Jung SC, Kim YJ. Placental gene expression is related to glucose metabolism and fetal cord blood levels of insulin and insulin-like growth factors in intrauterine growth restriction. Early Hum Dev. 2010 Jan;86(1):45–50.

32. Xiao X, Zhao Y, Jin R, Chen J, Wang X, Baccarelli A, et al. Fetal growth restriction and methylation of growth-related genes in the placenta. Epigenomics. 2016 Jan;8(1):33–42.

33. Tekola-Ayele F, Zeng X, Ouidir M, Workalemahu T, Zhang C, Delahaye F, et al. DNA methylation loci in placenta associated with birthweight and expression of genes relevant for early development and adult diseases. Clin Epigenetics. 2020 Dec;12(1):78.

34. Arama C, Quin JE, Kouriba B, Östlund Farrants AK, Troye-Blomberg M, Doumbo OK. Epigenetics and Malaria Susceptibility/Protection: A Missing Piece of the Puzzle. Front Immunol. 2018 Aug 3;9:1733.

35. Goldberg AD, Allis CD, Bernstein E. Epigenetics: A Landscape Takes Shape. Cell. 2007 Feb;128(4):635–8.

36. Dobbs KR, Embury P, Koech E, Ogolla S, Munga S, Kazura JW, et al. Age-related differences in monocyte DNA methylation and immune function in healthy Kenyan adults and children. Immun Ageing. 2021 Dec;18(1):11.

37. Romero DVL, Balendran T, Hasang W, Rogerson SJ, Aitken EH, Achuthan AA. Epigenetic and transcriptional regulation of cytokine production by Plasmodium falciparum-exposed monocytes. Sci Rep. 2024 Feb 5;14(1):2949.

38. Papageorghiou AT, Ohuma EO, Altman DG, Todros T, Ismail LC, Lambert A, et al. International standards for fetal growth based on serial ultrasound measurements: the Fetal Growth Longitudinal Study of the INTERGROWTH-21st Project. The Lancet. 2014 Sep;384(9946):869–79.

39. Yuan V, Hui D, Yin Y, Peñaherrera MS, Beristain AG, Robinson WP. Cell-specific characterization of the placental methylome. BMC Genomics. 2021 Dec;22(1):6.

40. Xu RH, Chen X, Li DS, Li R, Addicks GC, Glennon C, et al. BMP4 initiates human embryonic stem cell differentiation to trophoblast. Nat Biotechnol. 2002 Dec;20(12):1261–4.

41. Shi D, Zhou X, Cai L, Wei X, Zhang L, Sun Q, et al. Placental DNA methylation analysis of selective fetal growth restriction in monochorionic twins reveals aberrant methylated *CYP11A1* gene for fetal growth restriction. FASEB J. 2023 Oct;37(10):e23207.

42. Norton C, Clarke D, Holmstrom J, Stirland I, Reynolds PR, Jenkins TG, et al. Altered Epigenetic Profiles in the Placenta of Preeclamptic and Intrauterine Growth Restriction Patients. Cells. 2023 Apr 11;12(8):1130.

43. Lee S, Kim YN, Im D, Cho SH, Kim J, Kim JH, et al. DNA Methylation and gene expression patterns are widely altered in fetal growth restriction and associated with FGR development. Anim Cells Syst. 2021 May 4;25(3):128–35.

44. Monteagudo-Sánchez A, Sánchez-Delgado M, Mora JRH, Santamaría NT, Gratacós E, Esteller M, et al. Differences in expression rather than methylation at placenta-specific imprinted loci is associated with intrauterine growth restriction. Clin Epigenetics. 2019 Dec;11(1):35.

45. Papadatou I, Marinakis N, Botsa E, Tzanoudaki M, Kanariou M, Orfanou I, et al. Case Report: A Novel Synonymous ARPC1B Gene Mutation Causes a Syndrome of Combined Immunodeficiency, Asthma, and Allergy With Significant Intrafamilial Clinical Heterogeneity. Front Immunol. 2021 Feb 19;12:634313.

46. Du Q, Zhang M, Gao A, He T, Guo M. Epigenetic silencing *ZSCAN23* promotes pancreatic cancer growth by activating Wnt signaling. Cancer Biol Ther. 2024 Dec 31;25(1):2302924.

47. Batsukh T, Schulz Y, Wolf S, Rabe TI, Oellerich T, Urlaub H, et al. Identification and Characterization of FAM124B as a Novel Component of a CHD7 and CHD8 Containing Complex. Englert C, editor. PLoS ONE. 2012 Dec 21;7(12):e52640.

48. Care4Rare Canada Consortium, Choquet K, Tétreault M, Yang S, La Piana R, Dicaire MJ, et al. SPG7 mutations explain a significant proportion of French Canadian spastic ataxia cases. Eur J Hum Genet. 2016 Jul;24(7):1016–21.

49. Ismail MR, Ordi J, Menendez C, Ventura PJ, Aponte JJ, Kahigwa E, et al. Placental pathology in malaria: A histological, immunohistochemical, and quantitative study. Hum Pathol. 2000 Jan;31(1):85–93.

Figure 1.

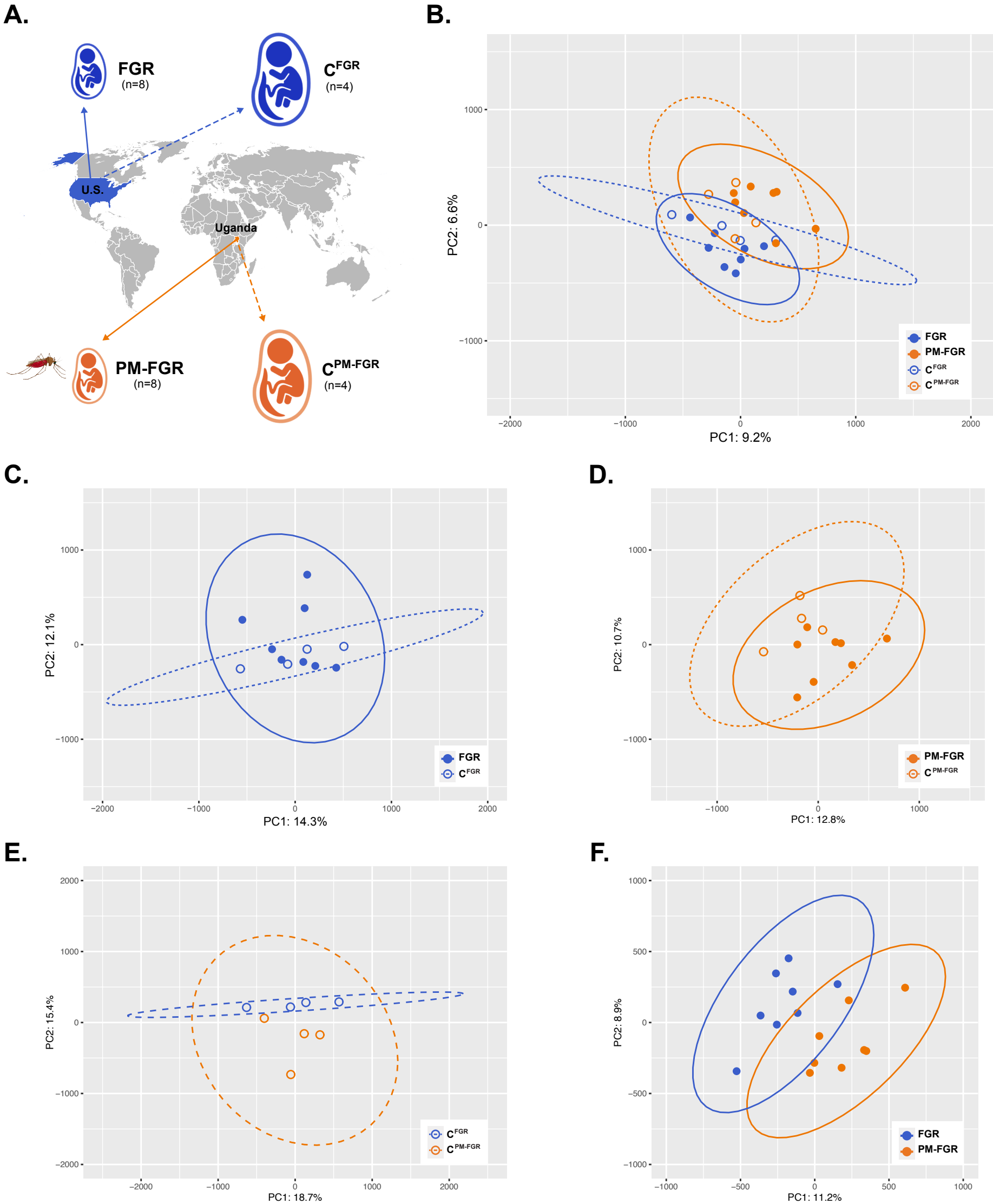
A.
FGR
(n=8)
C^FGR
(n=4)
U.S.
Uganda
PM-FGR
(n=8)
C^PM-FGR
(n=4)
B.
PC2: 6.6%
PC1: 9.2%
FGR
PM-FGR
C^FGR
C^PM-FGR
C.
PC2: 12.1%
PC1: 14.3%
FGR
C^FGR
D.
PC2: 10.7%
PC1: 12.8%
PM-FGR
C^PM-FGR
E.
PC2: 15.4%
PC1: 18.7%
C^FGR
C^PM-FGR
F.
PC2: 8.9%
PC1: 11.2%
FGR
PM-FGR

Figure 2.

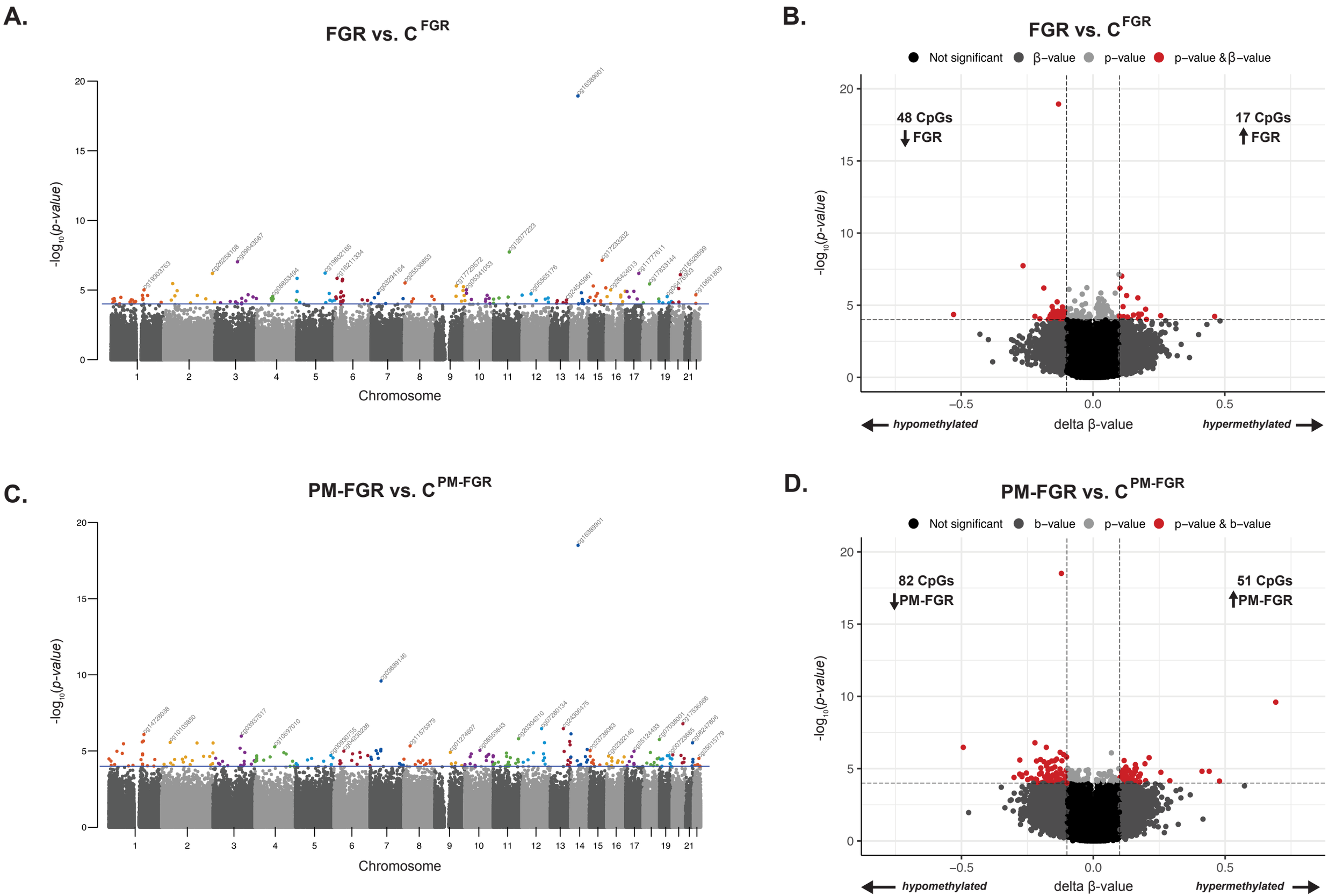
A.
FGR vs. C FGR
-log10(p-value)
Chromosome
B.
FGR vs. C FGR
Not significant
β–value
p–value
p–value & β–value
48 CpGs
FGR
17 CpGs
FGR
-log10(p-value)
hypomethylated
delta β-value
hypermethylated
C.
PM-FGR vs. C PM-FGR
-log10(p-value)
Chromosome
D.
PM-FGR vs. C PM-FGR
Not significant
b–value
p–value
p–value & b–value
82 CpGs
PM-FGR
51 CpGs
PM-FGR
-log10(p-value)
hypomethylated
delta β-value
hypermethylated

Figure 3.

A.

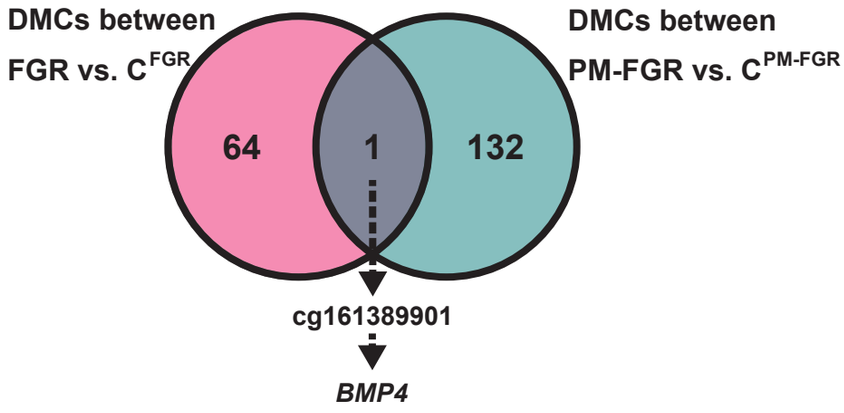
DMCs between
FGR vs. C^FGR
DMCs between
PM-FGR vs. C^PM-FGR
64
1
132
cg161389901
BMP4

B.

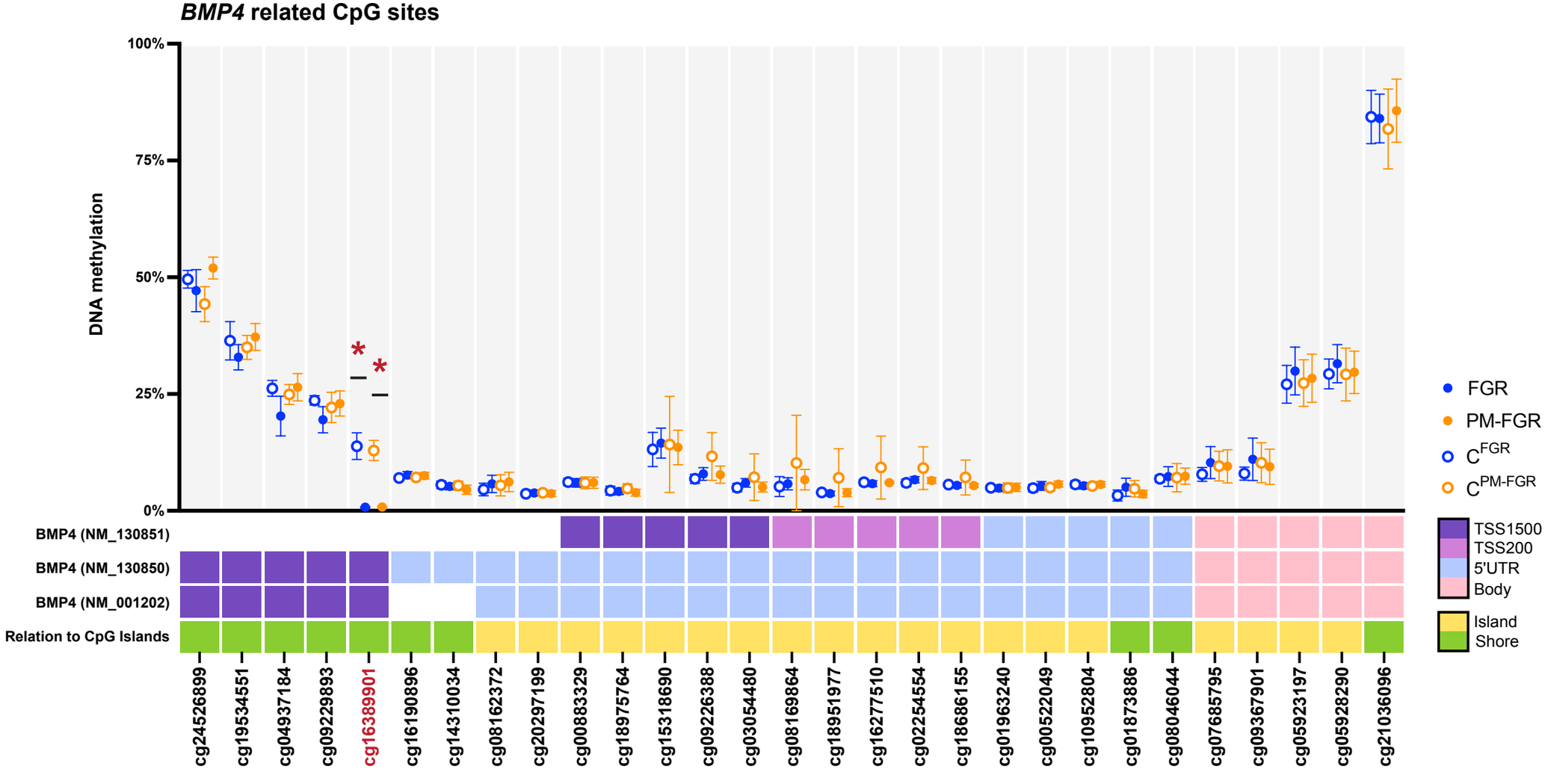
BMP4 related CpG sites
DNA methylation
100%
75%
50%
25%
0%
*
*
FGR
PM-FGR
C^FGR
C^PM-FGR
BMP4 (NM_130851)
BMP4 (NM_130850)
BMP4 (NM_001202)
Relation to CpG Islands
TSS1500
TSS200
5'UTR
Body
Island
Shore
cg24526899
cg19534551
cg04937184
cg09229893
cg16389901
cg16190896
cg14310034
cg08162372
cg20297199
cg00883329
cg18975764
cg15318690
cg09226388
cg03054480
cg08169864
cg18951977
cg16277510
cg02254554
cg18686155
cg01963240
cg00522049
cg10952804
cg01873886
cg08046044
cg07685795
cg09367901
cg05923197
cg05928290
cg21036096

Figure 4.

A.

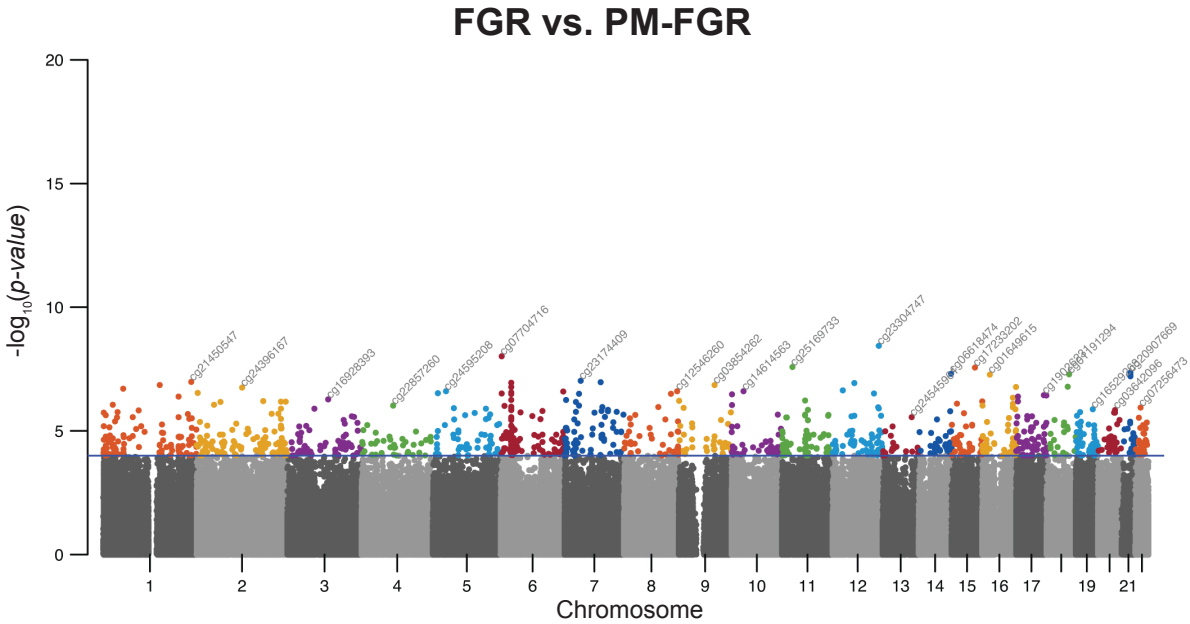
FGR vs. PM-FGR
-log10(p-value)
20
15
10
5
0
1
2
3
4
5
6
7
8
9
10
11
12
13
14
15
16
17
19
21
Chromosome

B.

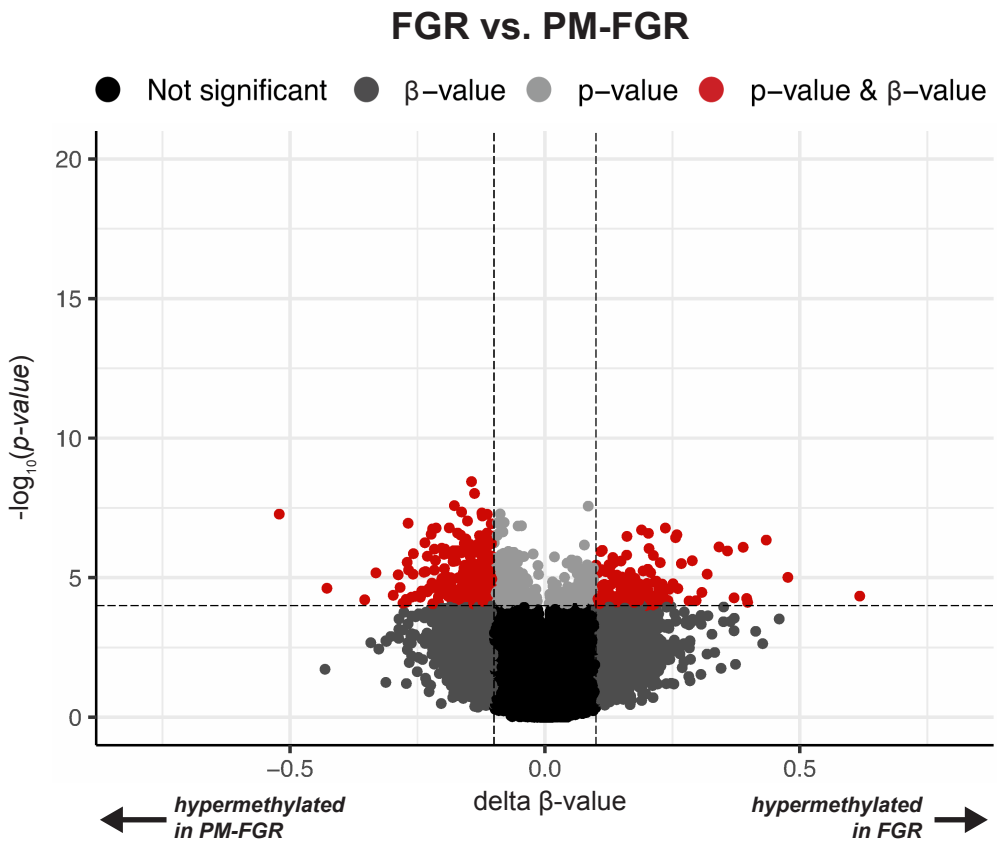
FGR vs. PM-FGR
Not significant
β–value
p–value
p–value & β–value
-log10(p-value)
20
15
10
5
0
–0.5
0.0
0.5
delta β-value
hypermethylated in PM-FGR
hypermethylated in FGR

C.

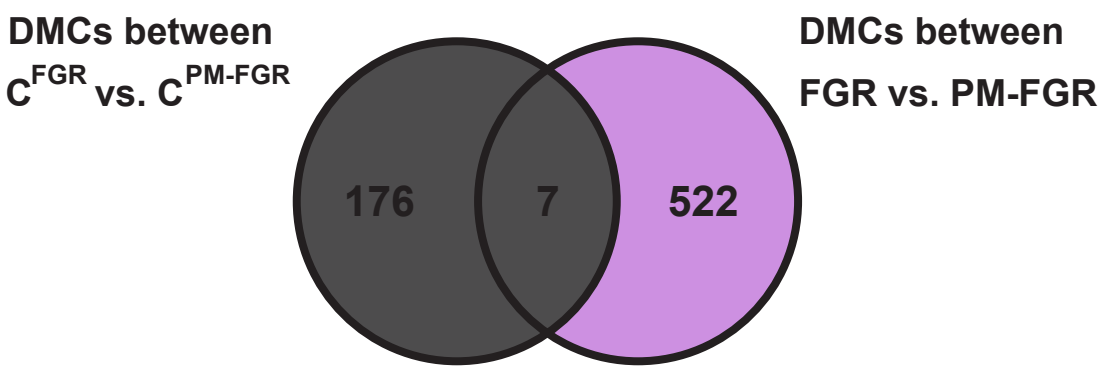
DMCs between
C^FGR vs. C^PM-FGR
DMCs between
FGR vs. PM-FGR
176
7
522

Figure 5.

A.

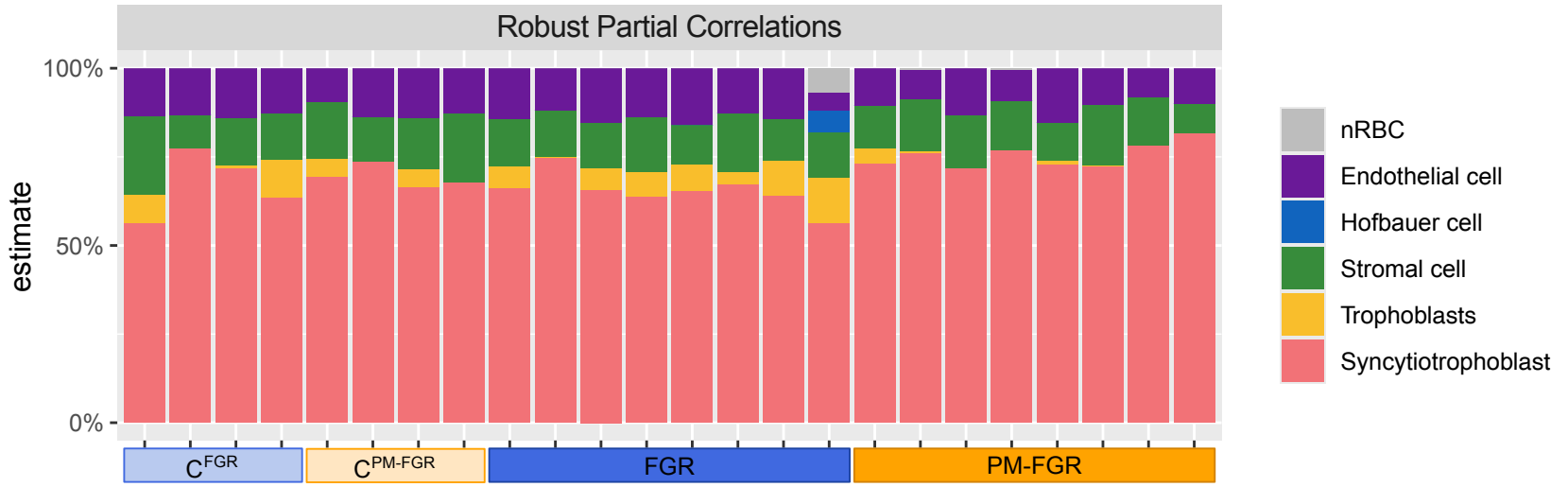

B.

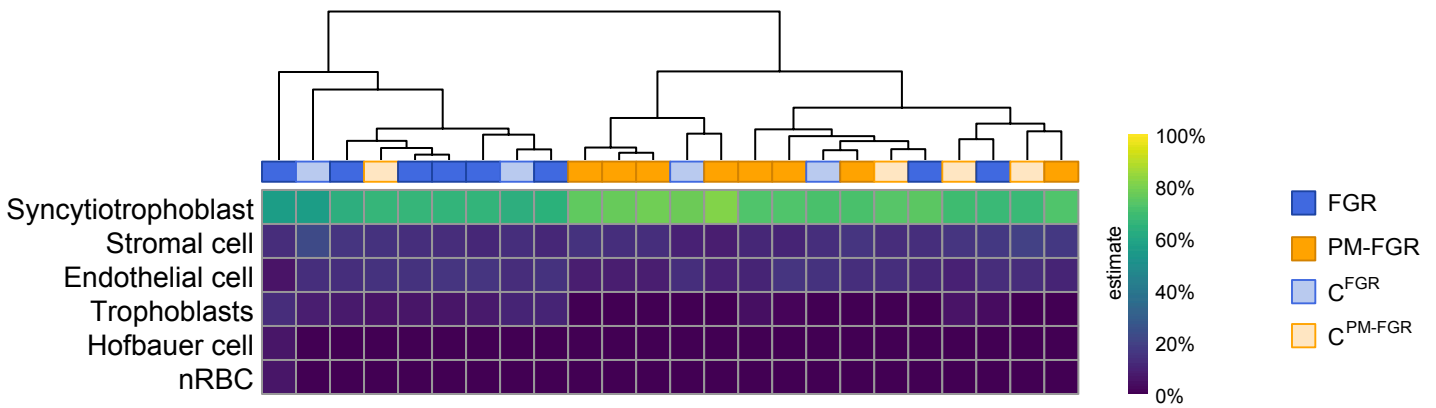

C.

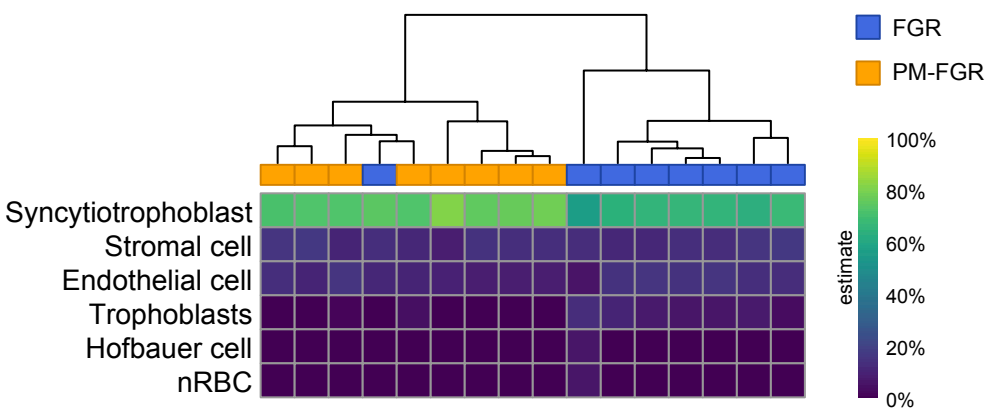
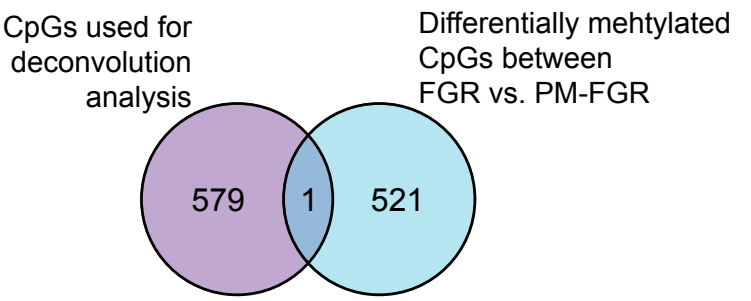
D.